NACA

RESEARCH MEMORANDUM

A SEMIEMPIRICAL CORRELATION OF AFTERBURNER COMBUSTION EFFICIENCY AND LEAN-BLOWOUT FUEL-AIR-RATIO DATA WITH SEVERAL AFTERBURNER-INLET VARIABLES AND AFTERBURNER LENGTHS

By Charles R. King

Lewis Flight Propulsion Laboratory
Cleveland, Ohio

NATIONAL ADVISORY COMMITTEE
FOR AERONAUTICS

WASHINGTON

September 17, 1957

NATIONAL ADVISORY COMMITTEE FOR AERONAUTICS

RESEARCH MEMORANDUM

A SEMIEMPIRICAL CORRELATION OF AFTERBURNER COMBUSTION EFFICIENCY AND LEAN-BLOWOUT FUEL-AIR-RATIO DATA WITH SEVERAL AFTERBURNER-INLET VARIABLES AND AFTERBURNER LENGTH

By Charles R. King

SUMMARY

A semiempirical correlation relating combustion efficiency with afterburner-inlet variables and length has been developed for a full-scale high-performance cylindrical turbojet afterburner using JP-4 fuel. The combustion efficiency in this correlation is expressed in terms of afterburner-inlet total temperature, total pressure, velocity, afterburner fuel-air ratio, and afterburner combustion-chamber length. The range of the parameters included in the correlation was as follows: total temperature, 1260° to 1860° R; total pressure, 750 to 1800 pounds per square foot absolute; velocity, 400 to 650 feet per second; fuel-air ratio, 0.034 to stoichiometric (0.0676); and combustion-chamber length, 2.5 to 5.5 feet. From the correlation, the predicted values of combustion efficiency were found to be within about ±5 percentage points of the experimental values of efficiency.

A correlation of the lean-blowout fuel-air-ratio data (for the same afterburner) was also obtained using the same afterburner-inlet parameters (total temperature, total pressure, and velocity) which correlated combustion efficiency. For a constant value of correlation parameter, the scatter of lean-blowout fuel-air ratio about the correlation curve was about ±0.003 unit of fuel-air ratio.

INTRODUCTION

Of the many processes taking place within a turbojet engine, the combustion process is probably the most difficult to comprehend. As a result, there is no completely adequate theoretical explanation of the combustion process. For this reason it is difficult to predict combustor performance.

[redacted]

In recent years, however, a concept has been developed that permits an empirical correlation of primary can-type combustor efficiency with some of the combustor-inlet variables (refs. 1 to 3). This concept is based on the assumption that the combustion efficiency is controlled by the rate of flame spreading through the combustor, and leads to an equation of the following type:

$$\eta_{AB} = f\left(\frac{p^{a}t^{b}}{V^{c}}\right) \tag{1}$$

(Symbols are defined in the appendix.)

An attempt is made in reference 4 to apply this correlation procedure to a gutter-type ram-jet combustor. Although a satisfactory correlation of the data was obtained, a comparison of the empirically determined exponents with theoretically predicted exponents in the equation (for inlet pressures above 1/2 atm) of reference 3 for a turbojet combustor shows that the exponents on afterburner-inlet temperature and pressure agree in both references, whereas the exponents for afterburner-inlet velocity do not.

The object of the investigation reported herein (which was conducted at the NACA Lewis laboratory) was to correlate the full-scale afterburner combustion-efficiency data of reference 5 by using the theory, parameters, and methods previously used in references 1 to 4, including the additional parameters of afterburner length and fuel-air ratio. (The data of ref. 5 were obtained on a full-scale high-performance afterburner configuration which was operated over a wide range of afterburner-inlet conditions with JP-4 fuel for several afterburner combustion-chamber lengths.) The exponents on the afterburner-inlet parameters were determined empirically and applied to data covering a range of fuel-air ratios from 0.0340 to 0.0676. An equation expressing afterburner combustion efficiency in terms of afterburner-inlet total temperature, total pressure, velocity, afterburner fuel-air ratio, and afterburner combustion-chamber length is presented herein.

A correlation of the afterburner lean-blowout fuel-air-ratio data using the same afterburner-inlet parameters (total temperature, total pressure, and velocity) and exponents that were determined for the combustion-efficiency correlation is also presented.

The semiempirical correlation of the afterburner combustion efficiency and lean-blowout fuel-air-ratio data presented herein includes data over the following range of conditions: afterburner-inlet total temperature, 1260° to 1860° R; afterburner-inlet total pressure, 750 to 1800 pounds per square foot absolute; afterburner-inlet velocity, 400 to 650 feet; afterburner fuel-air ratio, lean blowout to 0.0676; and afterburner combustion-chamber length, 2.5 to 5.5 feet.

APPARATUS AND PROCEDURE

Test Rig

The general layout of the full-scale afterburner test rig is presented in figure 1(a). Combustion air was supplied to the facility from the laboratory air system. Upon entering the facility, the combustion air was preheated to the desired afterburner-inlet temperature level by eight J35 turbojet combustors. The preheated air passed through a plenum chamber to assure flat temperature and velocity profiles at the inlet to the diffuser. An airflow measuring station was provided at the diffuser inlet. The instrumentation at this station, all other instrumentation stations, and a more complete description of the facility are given in detail in reference 5.

To prevent overheating, the shell was cooled by an external cooling shroud with air and water sprays installed inside the shroud space. The exhaust gases left the afterburner by passing through a choked exhaust nozzle. They were then cooled by water sprays downstream of the exhaust nozzle and discharged into the laboratory exhaust system.

Afterburner

The afterburner details are shown in figure 1(b). Complete dimensions and details of the afterburner and the variable-area exhaust nozzle are given in reference 5. The diffuser used in this investigation gave a relatively flat velocity profile at the diffuser exit. A single-manifold fuel system was used for this experimental program. The fuel-injection system (made up of 24 flattened spray bars installed 32 in. upstream of the flameholder) was developed to give a relatively flat fuel-air-ratio profile at the flameholder. The flameholder was a conventional, annular, V-gutter flameholder having 30-percent blockage and two $1\frac{1}{2}$-inch-wide gutters. In order to investigate the effects of length on afterburner performance, the afterburner length was varied in 1-foot increments from 2.5 to 5.5 feet. The afterburner combustion-chamber length is defined as the axial distance from the trailing edge of the flameholder to the effective nozzle throat (ref. 5). Afterburner ignition was accomplished with a torch igniter. All data were obtained without an internal cooling liner in the afterburner.

Operating Procedure

In general, the afterburner was systematically operated over a wide range of conditions during which the independent effects of afterburner fuel-air ratio, each afterburner-inlet variable, and afterburner length

on combustion efficiency and lean-blowout limits were determined. By means of the variable-area exhaust nozzle, it was possible to hold the afterburner-inlet conditions fixed as the afterburner fuel-air ratio was varied (from lean blowout to slightly higher than stoichiometric). A detailed discussion of the experimental operating procedure and of the basic data calculation procedure is included in reference 5.

CORRELATION EQUATION

The general equations previously developed and used in references 2 to 4 as a guide in correlating combustion-efficiency data is based on the assumption that the efficiency is controlled by the rate of flame spreading in the combustor (inasmuch as flame speed is one of the fundamental properties which can be used in a physical picture of the combustion process). A similar approach, based on the same assumptions but modified to apply to an afterburner, is outlined in the following paragraphs.

For this development the combustion process is visualized as the burning of combustible mixture zones of random size and shape, which are surrounded by a flame surface and which are consumed as they pass through the combustor. This picture of the combustion process was suggested by Wohlenberg in reference 6 and is used in the analyses of references 2 and 3 to obtain satisfactory correlations of primary engine combustor data. A simplified expression for combustion efficiency, which is based on this model of the combustion process and appears in reference 4 (eq. (1)), is as follows:

$$\eta_{AB} = \frac{A_f U_f}{A_r V_r} \tag{2}$$

The numerator of equation (2) is proportional to the rate of consumption of the combustible mixture in the combustor; the denominator is proportional to the rate of flow of the combustible mixture through the combustor. Because the velocity approaching the flame front varies from the flameholder to the point at which the flame front intersects the wall or another flame front, the reference velocity V_r is an effective, rather than an actual, velocity approaching the flame front. This effective velocity is assumed to be a function of the afterburner-inlet velocity V only. The reference area A_r is the effective flame-front area from the flameholder to the point at which the flame front intersects the wall or another flame front. The effective area is assumed to equal the product of the afterburner cross-sectional area and a function of the afterburner-inlet velocity. By applying these considerations to equation (2),

$$\eta_{AB} = \frac{A_f U_f}{A_{AB} f_1(V)} \tag{3}$$

[redacted]

The combustible mixture zones of random size and shape in the combustor, which are surrounded by a flame surface and consumed as they pass through the combustor, are assumed to have the same surface-to-volume ratio at any point in the combustor as at the beginning of the combustion process (i.e., along the flame front). Thus,

$$\frac{A_f}{v} = \frac{A_{f,i}}{v_i} \tag{4}$$

The initial flame surface per unit volume of combustor $A_{f,i}/v_i$ is shown in reference 6 to be a function of the over-all fuel-air ratio, the combustor geometry, and the combustor-inlet conditions. The expression, similar to that presented in reference 2, which relates these variables is as follows:

$$\frac{A_{f,i}}{v_i} = DK_1\left(\frac{p}{t}\right)^{0.333}(Re)^a(Pr)^b f_2\left(\frac{f}{a}\right)_{AB} \tag{5}$$

Although the number of combustible mixture zones within the afterburner is greatest at the flameholder and varies along the combustor, the volume of the combustible mixture zones in the combustor can be associated mainly with the rate of energy release along the combustor, which, in turn, is equal to the product of the volume of the combustor and a function of the combustion efficiency. Thus,

$$v = v_{AB} f_3(\eta_{AB}) \tag{6}$$

Substituting equations (5) and (6) in equation (4) gives

$$A_f = DK_1\left(\frac{p}{t}\right)^{0.333}(Re)^a(Pr)^b\left[f_2\left(\frac{f}{a}\right)_{AB}\right]\left[f_3(\eta_{AB})\right](v_{AB}) \tag{7}$$

wherein (as in refs. 2 and 3) the effects of both Reynolds number and Prandtl number are assumed to be negligible. Substituting the following empirical relation for maximum flame speed (as in refs. 2 to 4):

$$U_f = K_2 t^{1.4} \tag{8}$$

and equation (7) in equation (3) and rearranging terms give

$$f_4(\eta_{AB}) = \frac{K_3 D\left(\frac{p}{t}\right)^{0.333}\left[f_2\left(\frac{f}{a}\right)_{AB}\right] v_{AB} t^{1.4}}{A_{AB} f_1(V)} \tag{9}$$

Combining like terms in equation (9) yields

$$f_4(\eta_{AB}) = K_3 Dp^{0.333} t^{1.07} f_2(f/a)_{AB} f_5(V) \qquad (10)$$

Equation (10) involves the use of static pressures and temperatures. The work presented herein makes use of measured total rather than static afterburner-inlet pressures and temperatures because the total measurements were determined to be more reliable. (Check correlations indicated there would be no discrepancies introduced into the correlation by this procedure in the range of conditions investigated (max. afterburner-inlet Mach number was about 0.38).)

4552

DETERMINATION OF EXPONENTIAL RELATIONS AND EVALUATION OF EQUATION

An inspection of equation (10) reveals the fact that it is not possible to determine directly absolute values of the exponents on the temperature and pressure parameters included in the equation; however, the ratio between the exponents of these two parameters can be determined. This is accomplished by plotting temperature against pressure on logarithmic coordinates with all other parameters (including combustion efficiency) held constant. The reciprocal of the slope of the curve on the logarithmic plot represents the ratio of the exponents of the parameters plotted. The next step in the procedure will be to determine empirically the form of the remaining variables which will give a satisfactory correlation of the data of reference 5. This will be done by plotting each of these parameters against both the temperature and the pressure with all other variables held constant.

Afterburner-Inlet Total Temperature and Total Pressure

Figure 2 presents a log-log plot for a typical set of conditions showing the exponential relation between afterburner-inlet total temperature and total pressure. For the conditions presented, the slope (which is equal to the ratio of the pressure exponent to the temperature exponent) of the curves is equal to 0.303. This compares favorably with a value of 0.311 predicted by equation (10) and values of 0.3 and 0.292, which satisfactorily correlate the data in references 3 and 4, respectively. An equation representing the relation between afterburner-inlet total temperature and total pressure, therefore, might be written as follows:

$$f_4(\eta_{AB}) = T^a P^{0.303a} f_6\left[(f/a)_{AB} V\right] \qquad (11)$$

[redacted]

Afterburner-Inlet Velocity

In order to determine the form of the velocity parameter which will give the most satisfactory correlation of the data of reference 5, several trial plots were made involving various forms of this parameter. An examination of these plots indicated that a satisfactory correlation might be obtained by using the expression (750 - V). In figure 3 data are plotted using the afterburner-inlet velocity parameter in the form of (750 - V) to show the straight-line relation which was obtained.

An equation representing the relation between the newly determined afterburner-inlet velocity parameter and the temperature and pressure parameters is as follows:

$$f_4(\eta_{AB}) = T^{a}P^{0.303a}(750 - V)^{0.236a}f_7\left[(f/a)_{AB}l\right] \tag{12}$$

Afterburner Combustion-Chamber Length

A situation similar to that for inlet velocity was found to exist for the variable combustion-chamber length. After extensive trial plotting, it was determined that semilog plots of the afterburner-inlet parameters (total temperature, total pressure, and (750 - V)) against the reciprocal of the afterburner combustion-chamber length $1/l$ provided the most satisfactory representation of the data of reference 5. Such a plot is shown in figure 4. The curves represent average slopes obtained from all the data of reference 5. Thus, a general correlating equation can now be written which will include the afterburner-inlet parameters, total temperature, total pressure, and (750 - V), and the afterburner combustion-chamber length:

$$f_4(\eta_{AB}) = \frac{T^{a}P^{0.303a}(750 - V)^{0.236a}}{e^{\left(\frac{2.78a}{l}\right)}} f_8\left(\frac{f}{a}\right)_{AB} \tag{13}$$

COMBUSTION-EFFICIENCY CORRELATION

The final step in the determination of the over-all correlation parameter, ξ, which will be used to correlate the combustion-efficiency data, is the assignment of absolute values to the exponents of each of the individual parameters. An absolute value was arbitrarily assigned to the exponent on the afterburner-inlet total temperature which was consistent with the exponent value of equation (10). The remaining exponents were then determined from equation (13). The resulting expression for the correlating parameter ξ is thus given by the following equation:

$$\xi = \frac{P^{0.324} T^{1.07} (750 - V)^{0.252}}{e^{3/l}} \tag{14}$$

The resulting plots of combustion efficiency against ξ for four nominal values of fuel-air ratio (0.0663, 0.055, 0.0465, and 0.036) are presented in figures 5(a), (b), (c), and (d), respectively, and include the actual data points from which the crossplots of reference 5, which were obtained over wide ranges of afterburner-inlet conditions and for several afterburner combustion-chamber lengths, were constructed. The data are keyed for afterburner-inlet temperatures and pressures and include data for afterburner combustion-chamber lengths from 2.5 to 5.5 feet and afterburner-inlet velocities from 400 to 650 feet per second. The accuracy of this correlation is seen to be about ±5 percentage points in combustion efficiency, which is not substantially greater than the probable mean error in the original data.

The curves presented in figures 5(a) to (d) are summarized in figure 5(e). Although the curves of figure 5(e) provide a useful correlation of all the data, an examination of this figure indicates the curves for the four levels of fuel-air ratio are similar in shape but displaced slightly from one another. The similarity of the curves indicated that there was a good possibility of obtaining a single correlation of the data for the four fuel-air ratios, and thus attempts were made to do this. As a result of making many trial plots, it was found that, when the curves of figure 5(e) were replotted on log-log coordinates, they could be closely approximated by straight lines. The general equation for these straight lines was determined to be as follows:

$$\frac{1 - \eta_{AB}}{\eta_{AB}} = I\left(\frac{10{,}000}{\xi} - 0.09\right)^{m} \tag{15}$$

where I represents the intercept and m, the slope of each straight line. It was found that the slopes and the intercepts of the straight-line curves varied linearly with the functions of afterburner fuel-air ratio or equivalence ratio φ as follows:

$$m = 1.119(1 - \varphi)^2 + 1.845 \tag{16}$$

$$I = 270.6(1 - \varphi)^3 + 16.20 \tag{17}$$

These expressions can be substituted in equation (15) to give a semi-empirical correlation equation:

$$\frac{1 - \eta_{AB}}{\eta_{AB}} = \left[270.6(1 - \varphi)^3 + 16.20\right]\left(\frac{10{,}000}{\xi} - 0.09\right)^{1.119(1-\varphi)^2+1.845} \tag{18}$$

where ξ is defined in equation (14).

[redacted]

An indication of the over-all accuracy of the semiempirical equation was obtained by comparing measured with computed values of combustion efficiency. The comparison is presented in figure 6 for all afterburner-inlet total temperatures, total pressures, velocities, and afterburner combustion-chamber lengths investigated in reference 5, and for afterburner fuel-air ratios from 0.034 to 0.0676. Most of the data in this final correlation fall within ±5 percentage points of the predicted value of combustion efficiency, and thus the equation is felt to be within the estimated accuracy of the measured values.

LEAN-BLOWOUT CORRELATION

In figure 7 an attempt is made to correlate the lean-blowout data of reference 5 using the afterburner-inlet parameters, pressure, temperature and (750 - V), along with their corresponding empirical exponents, which successfully correlated the combustion efficiency. The data are presented for a wide range of afterburner-inlet conditions and have been keyed for afterburner combustion-chamber length. Although the variations with afterburner-inlet conditions were random, figure 7 indicates that there may be some small effect of length on lean-blowout fuel-air ratio; however, these variations are within the estimated accuracy of the data, that is, about ±0.003 unit of fuel-air ratio (ref. 5).

SUMMARY OF RESULTS

A semiempirical correlation and equation were obtained relating the combustion efficiency of a cylindrical turbojet afterburner to several afterburner-inlet parameters and afterburner lengths. The range of the parameters included in the correlation was as follows: total temperature, 1260° to 1860° R; total pressure, 750 to 1800 pounds per square foot absolute; velocity, 400 to 650 feet per second; afterburner fuel-air ratio, 0.034 to stoichiometric (0.0676); and afterburner length, 2.5 to 5.5 feet. The correlation included herein was developed from data obtained on a high-performance afterburner using JP-4 fuel. The diffuser installed in this afterburner was designed to give a flat velocity profile at the inlet to the afterburner. Flattened radial fuel bars designed to produce a flat fuel-air distribution at the inlet to the afterburner were installed in the diffuser annulus 32 inches upstream of a 30-percent-blockage flameholder, which was made of two $1\frac{1}{2}$-inch-wide annular V-gutters.

The concepts and procedures used to obtain the correlation were similar to those used to correlate primary combustor data. The accuracy of the correlation is about ±5 percentage points of the predicted value of combustion efficiency, which is not substantially greater than the probable mean error in the original data.

An empirical correlation of the lean-blowout fuel-air-ratio data was obtained by using the same afterburner-inlet parameters (pressure, temperature, and velocity) which correlated combustion efficiency. The variation in the correlation of the lean-blowout fuel-air-ratio data was about ±0.003 unit of afterburner fuel-air ratio.

Lewis Flight Propulsion Laboratory
National Advisory Committee for Aeronautics
Cleveland, Ohio, July 5, 1957

APPENDIX - SYMBOLS

A_{AB}	cross-sectional area of afterburner combustion chamber, sq ft
A_f	total flame surface area in combustor, sq ft
$A_{f,i}$	initial flame surface area, sq ft
A_r	effective flame-front area, sq ft
a, b, c	exponents
D	characteristic dimension of combustor, ft
$f_1, f_2, \ldots$	functions
$(f/a)_{AB}$	afterburner fuel-air ratio
I	empirical intercept
$K_1, K_2, \ldots$	constants
l	afterburner combustion-chamber length, ft
m	empirical exponent
P	afterburner-inlet total pressure, lb/sq ft abs
Pr	Prandtl number
p	afterburner-inlet static pressure, lb/sq ft abs
Re	Reynolds number
T	afterburner-inlet total temperature, $^{\circ}R$
t	afterburner-inlet static temperature, $^{\circ}R$
U_f	maximum flame speed, ft/sec
V	afterburner-inlet velocity, ft/sec
V_r	effective velocity approaching flame front based on A_r, ft/sec
v	total volume of combustible mixture zones, cu ft

[redacted]

V_{AB}	volume of afterburner combustion chamber, cu ft
V_i	initial volume of combustible mixture zones, cu ft
η_{AB}	afterburner combustion efficiency
$\varkappa$	lean-blowout fuel-air-ratio correlation parameter
ξ	combustion-efficiency correlation parameter
φ	equivalence ratio, $\frac{(f/a)_{AB}}{0.0676}$

REFERENCES

1. Childs, J. Howard: Preliminary Correlation of Efficiency of Aircraft Gas-Turbine Combustors for Different Operating Conditions. NACA RM E50F15, 1950.

2. Graves, Charles C.: Effect of Oxygen Concentration of the Inlet Oxygen-Nitrogen Mixture on the Combustion Efficiency of a Single J33 Turbojet Combustor. NACA RM E52F13, 1952.

3. Childs, J. Howard, and Graves, Charles C.: Relation of Turbine-Engine Combustion Efficiency to Second-Order Reaction Kinetics and Fundamental Flame Speed. NACA RM E54G23, 1954.

4. Reynolds, Thaine W., and Ingebo, Robert D.: Combustion Efficiency of Homogeneous Fuel-Air Mixtures in a 5-Inch Ram-Jet Type Combustor. NACA RM E52I23, 1952.

5. King, Charles R.: Experimental Investigation of Effects of Combustion-Chamber Length and Inlet Total-Temperature, Total Pressure, and Velocity on Afterburner Performance. NACA RM E57C07, 1957.

6. Wohlenberg, W. J.: The Influence of Reaction Interface Extension in the Combustion of Gaseous Fuel Constituents. Trans. ASME, vol. 70, no. 3, Apr. 1948, pp. 143-156; discussion, pp. 156-160.

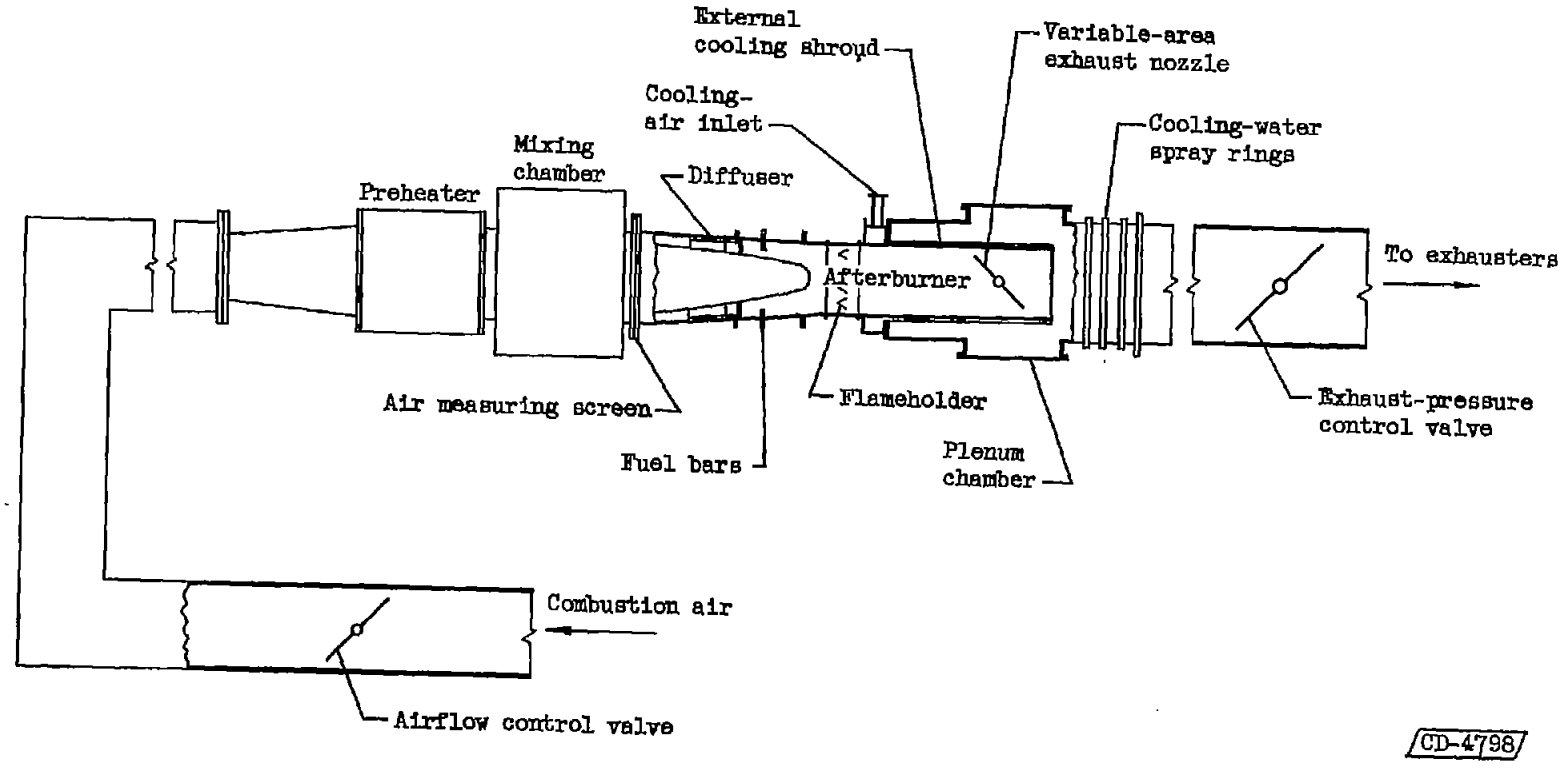

(a) Test rig.

Figure 1. - Schematic diagram of simulated afterburner test rig and afterburner.

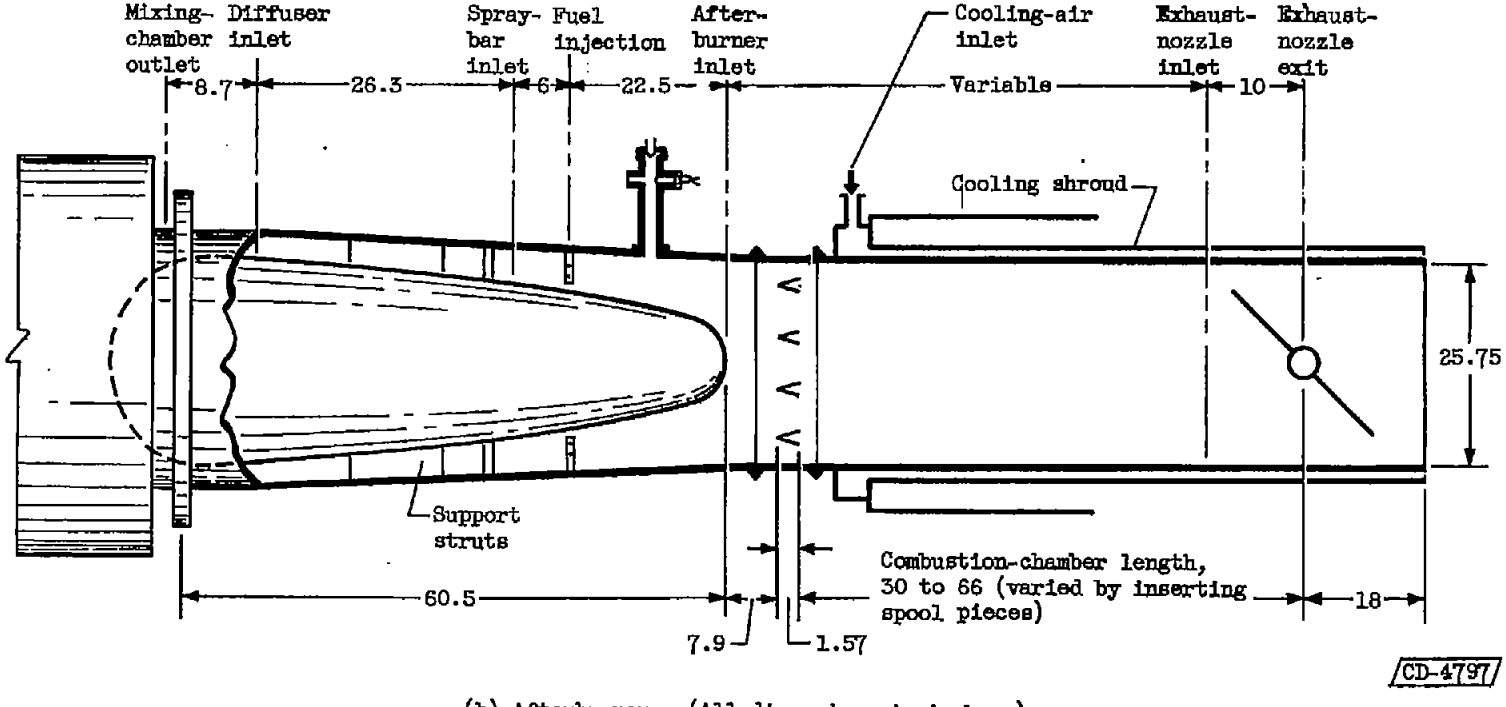

(b) Afterburner. (All dimensions in inches.)

Figure 1. - Concluded. Schematic diagram of simulated afterburner test rig and afterburner.

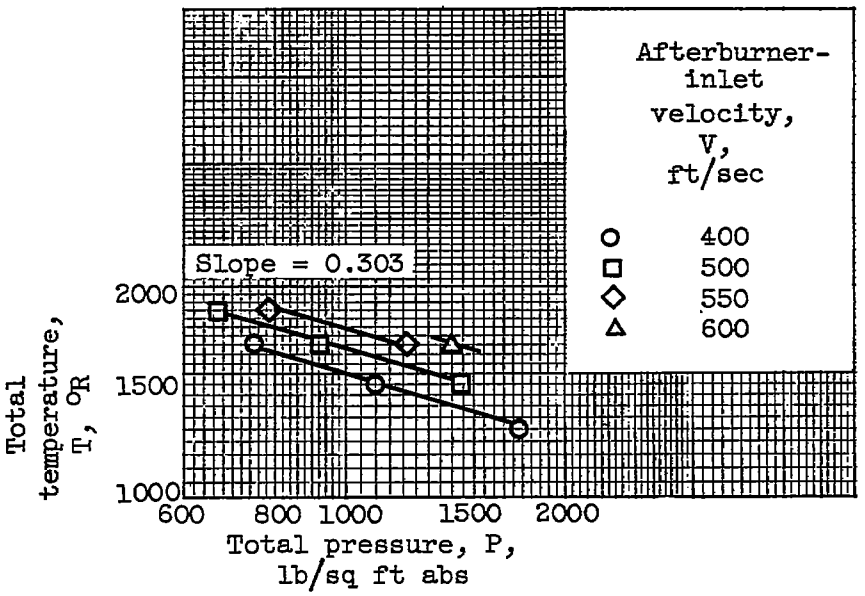

Figure 2. - Typical exponential relation between afterburner-inlet total pressure and total temperature for several velocities. Afterburner combustion efficiency, 70 percent; afterburner length, 3.33 feet; afterburner fuel-air ratio, 0.055.

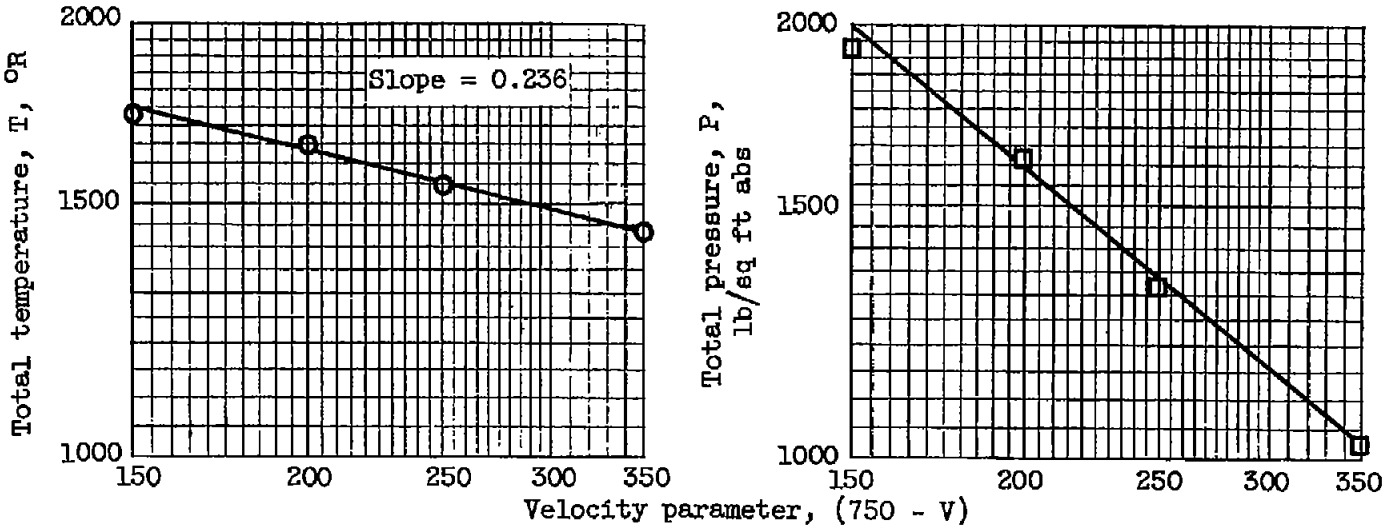

(a) Afterburner-inlet total temperature; afterburner-inlet total pressure, 1200 pounds per square foot absolute.

(b) Afterburner-inlet total pressure; afterburner-inlet total temperature, 1500° R.

Figure 3. - Typical exponential relations between afterburner velocity parameter (750 - V) and several afterburner parameters. Afterburner combustion efficiency, 70 percent; afterburner fuel-air ratio, 0.055; afterburner combustion-chamber length, 3.33 feet.

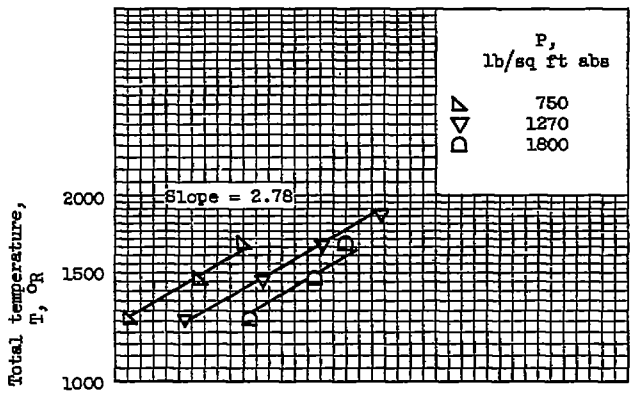

(a) Afterburner-inlet total temperature; afterburner-inlet velocity, 400 feet per second.

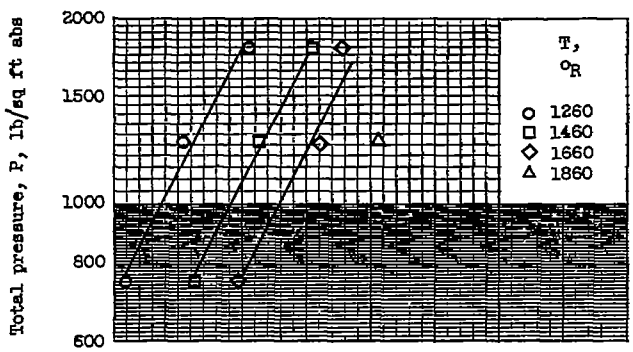

(b) Afterburner inlet total pressure; afterburner-inlet velocity, 400 feet per second.

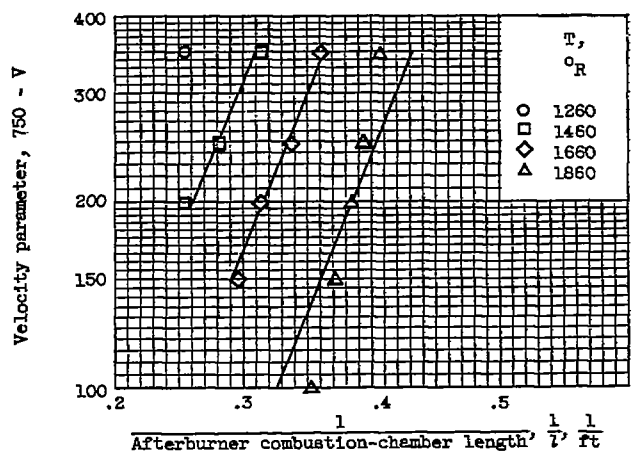

(c) Afterburner-inlet velocity parameter; afterburner-inlet total pressure, 1270 pounds per square foot absolute.

Figure 4. - Typical exponential relation between both afterburner-inlet total temperature and pressure and afterburner combustion-chamber length. Afterburner combustion efficiency, 70 percent; afterburner fuel-air ratio, 0.055.

[redacted]

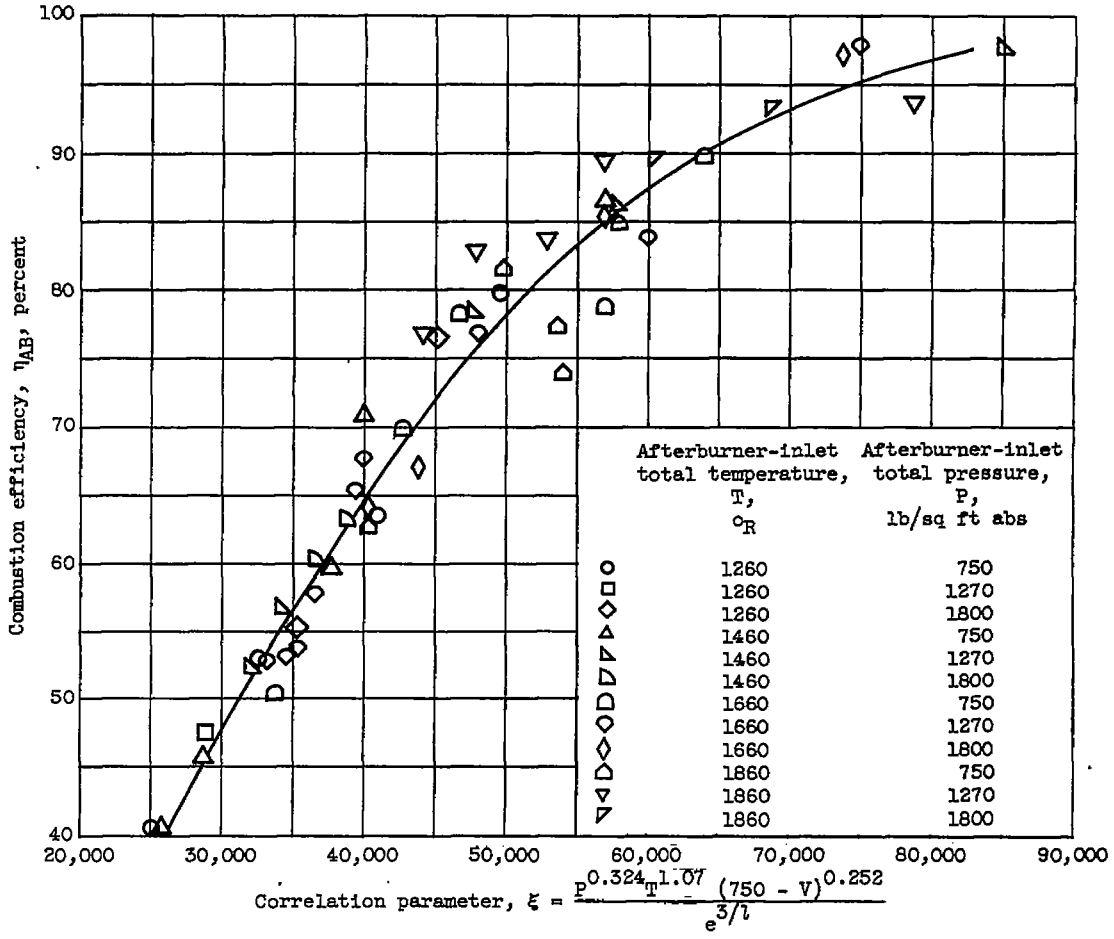

(a) Afterburner fuel-air ratio, 0.0663.

Figure 5. - Correlation of afterburner combustion-efficiency data for range of afterburner temperatures and pressures. Velocity, 400 to 650 feet per second; afterburner combustion-chamber length, 2.5 to 5.5 feet.

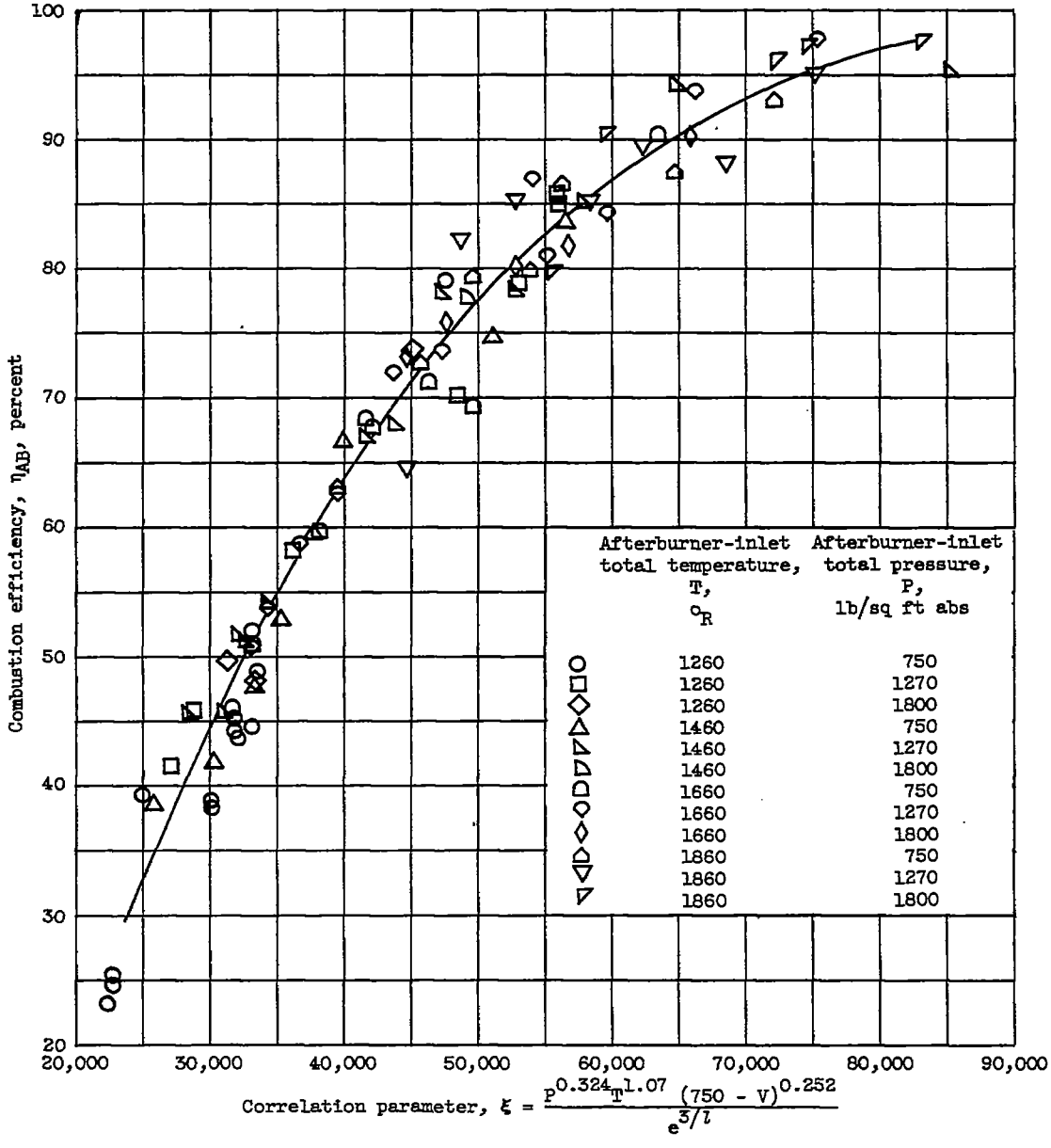

(b) Afterburner fuel-air ratio, 0.055.

Figure 5. - Continued. Correlation of afterburner combustion-efficiency data for range of afterburner temperatures and pressures. Velocity, 400 to 650 feet per second; afterburner combustion-chamber length, 2.5 to 5.5 feet.

[redacted]

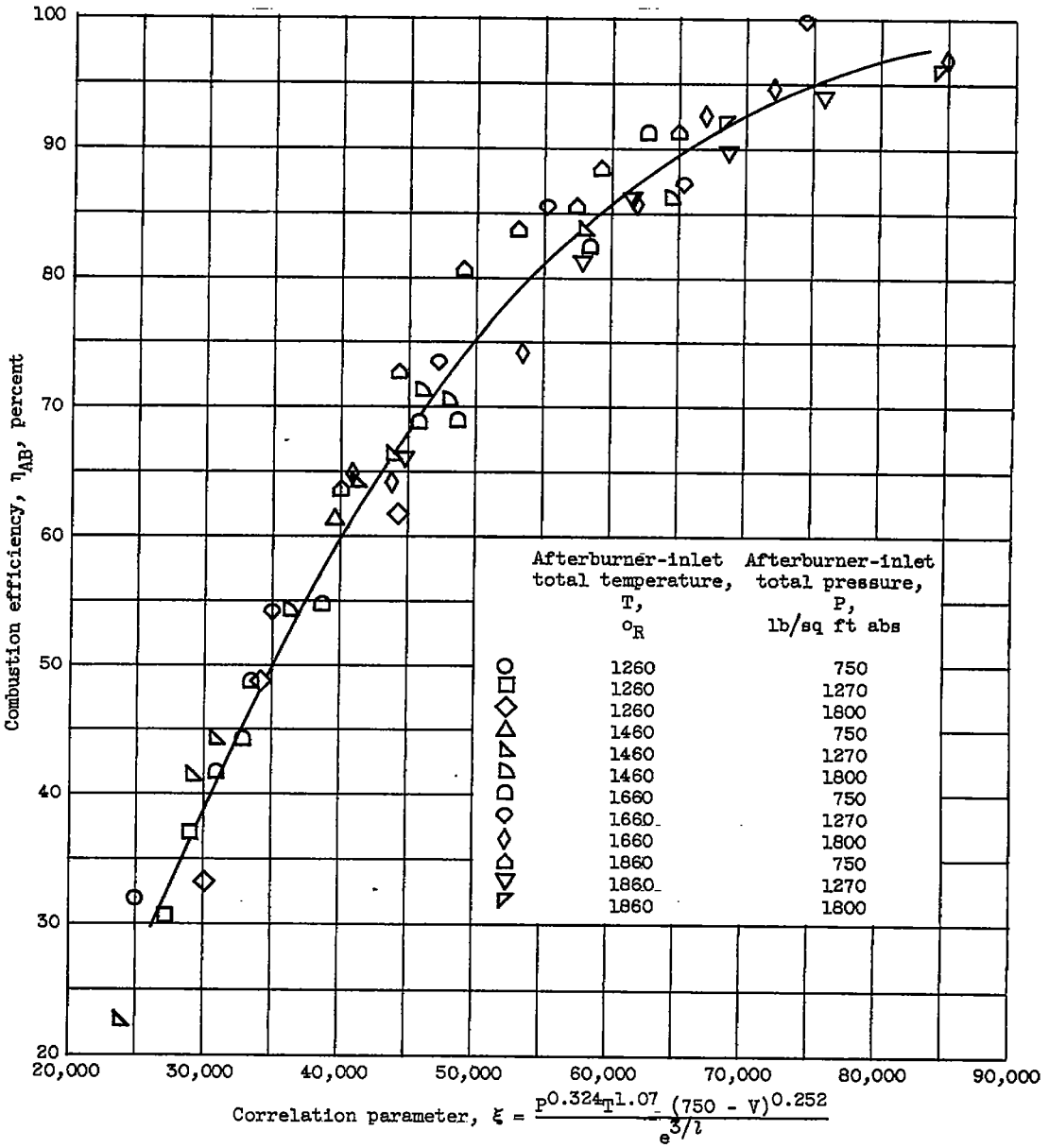

(c) Afterburner fuel-air ratio, 0.0465.

Figure 5. - Continued. Correlation of afterburner combustion-efficiency data for range of afterburner temperatures and pressures. Velocity, 400 to 650 feet per second; afterburner combustion-chamber length, 2.5 to 5.5 feet.

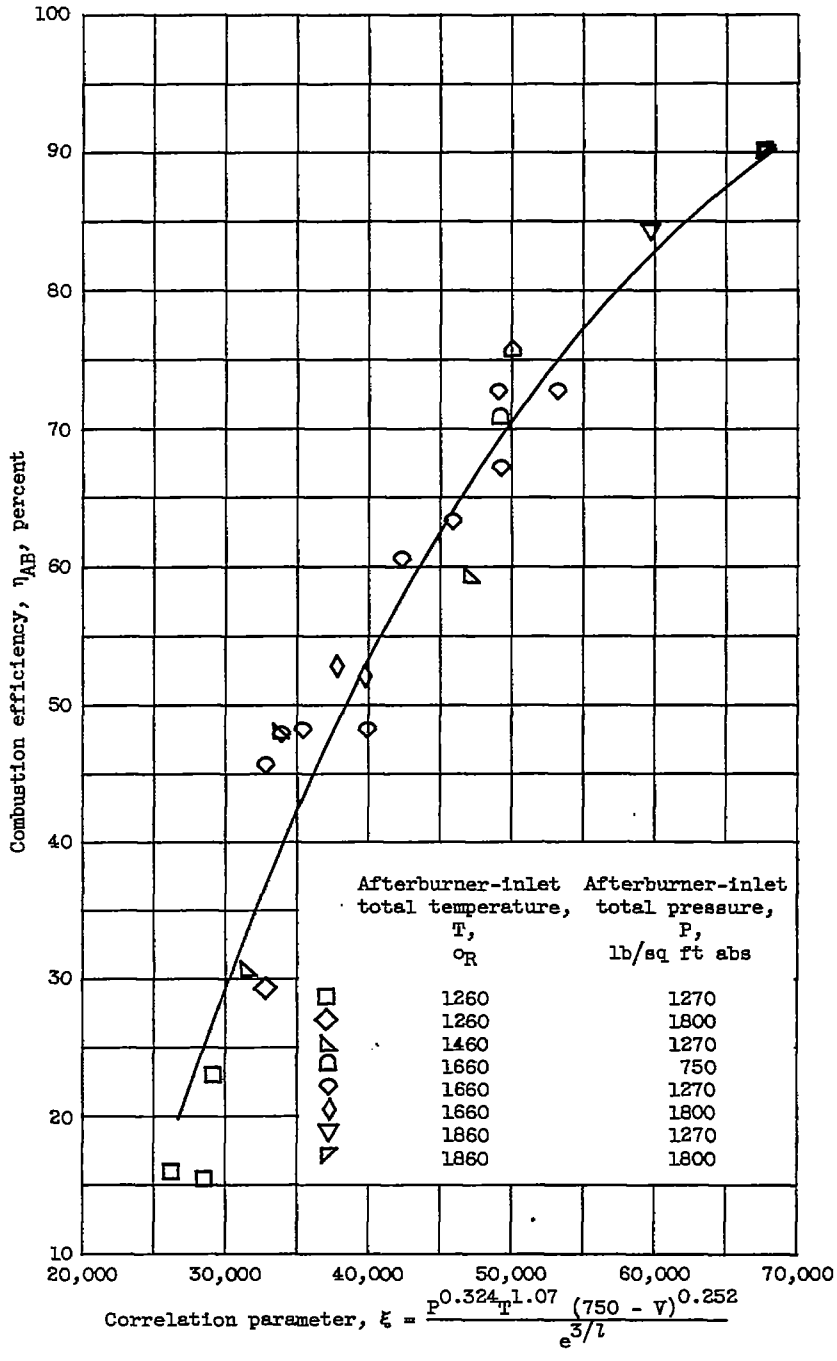

(d) Afterburner fuel-air ratio, 0.036.

Figure 5. - Continued. Correlation of afterburner combustion-efficiency data for range of afterburner temperatures and pressures. Velocity, 400 to 650 feet per second; afterburner combustion-chamber length, 2.5 to 5.5 feet.

[redacted]

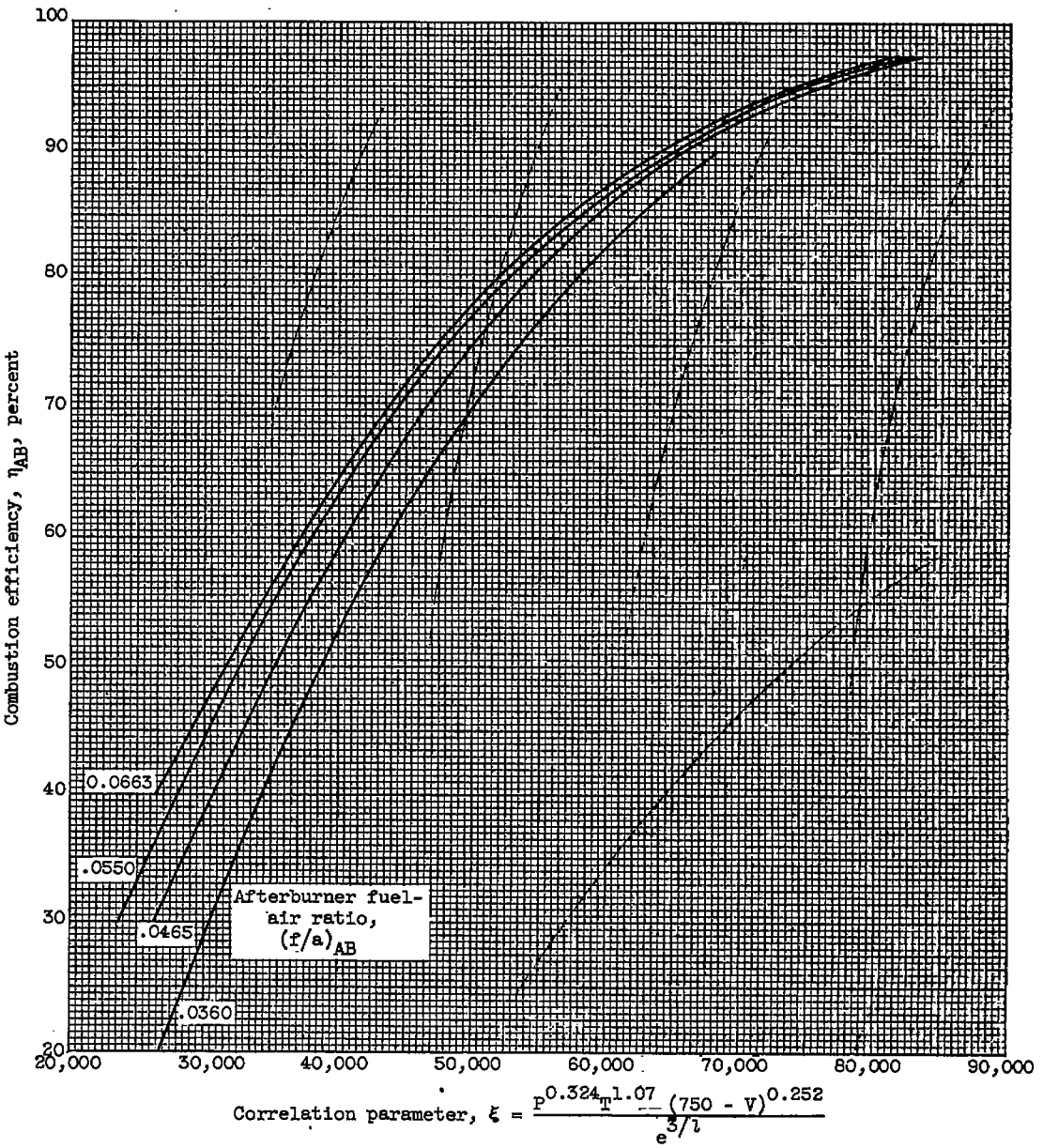

(e) Afterburner fuel-air ratios, 0.036 to 0.0663.

Figure 5. - Concluded. Correlation of afterburner combustion-efficiency data for range of afterburner temperatures and pressures. Velocity, 400 to 650 feet per second; afterburner combustion-chamber length, 2.5 to 5.5 feet.

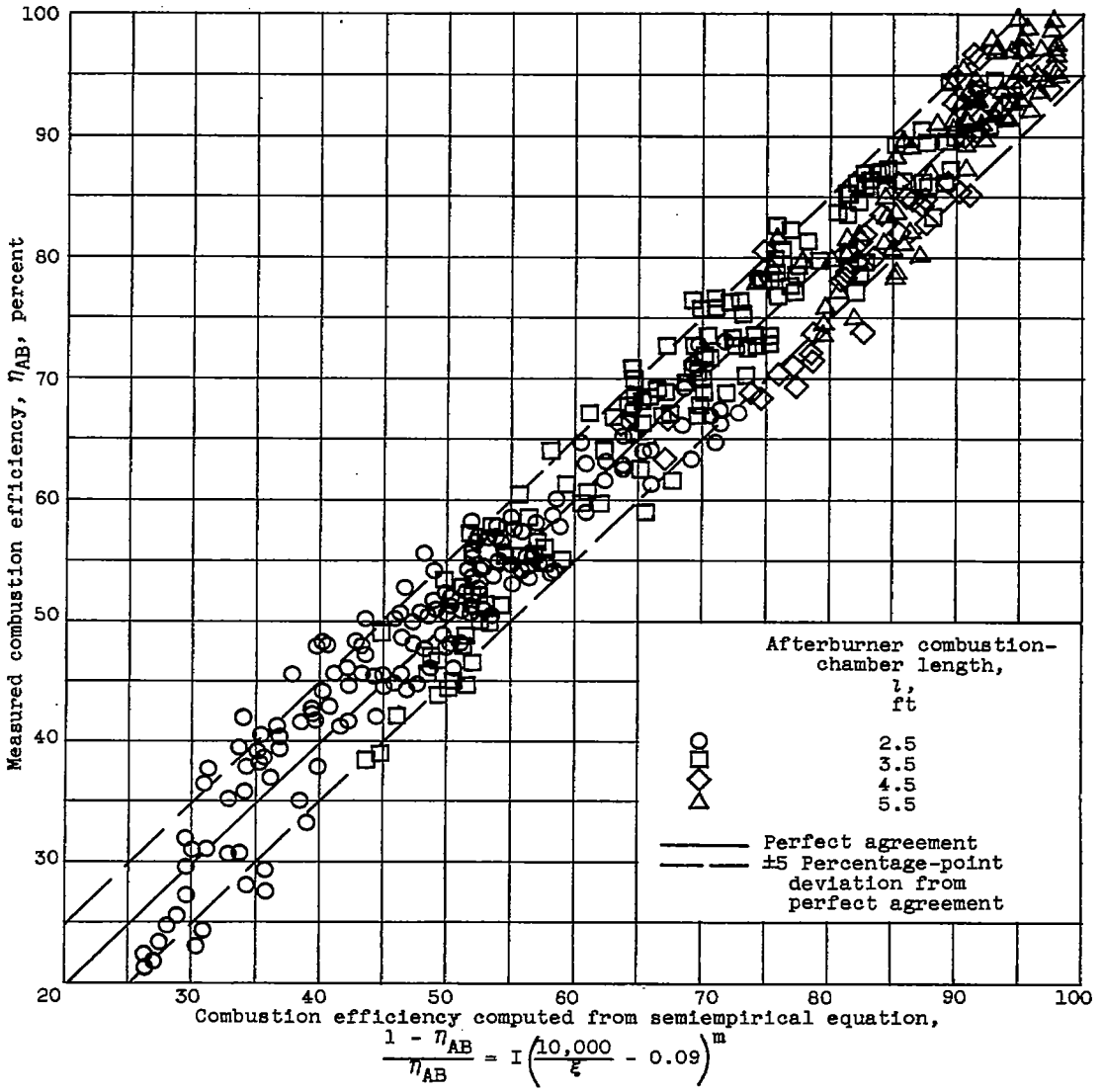

Figure 6. - Comparison of measured combustion efficiency with efficiency computed from semiempirical equation. Afterburner-inlet total temperatures, 1260° to 1860° R; afterburner-inlet total pressures, 750 to 1800 pounds per square foot absolute; afterburner-inlet velocities, 400 to 650 feet per second; fuel-air ratios, 0.034 to 0.0676.

[redacted]

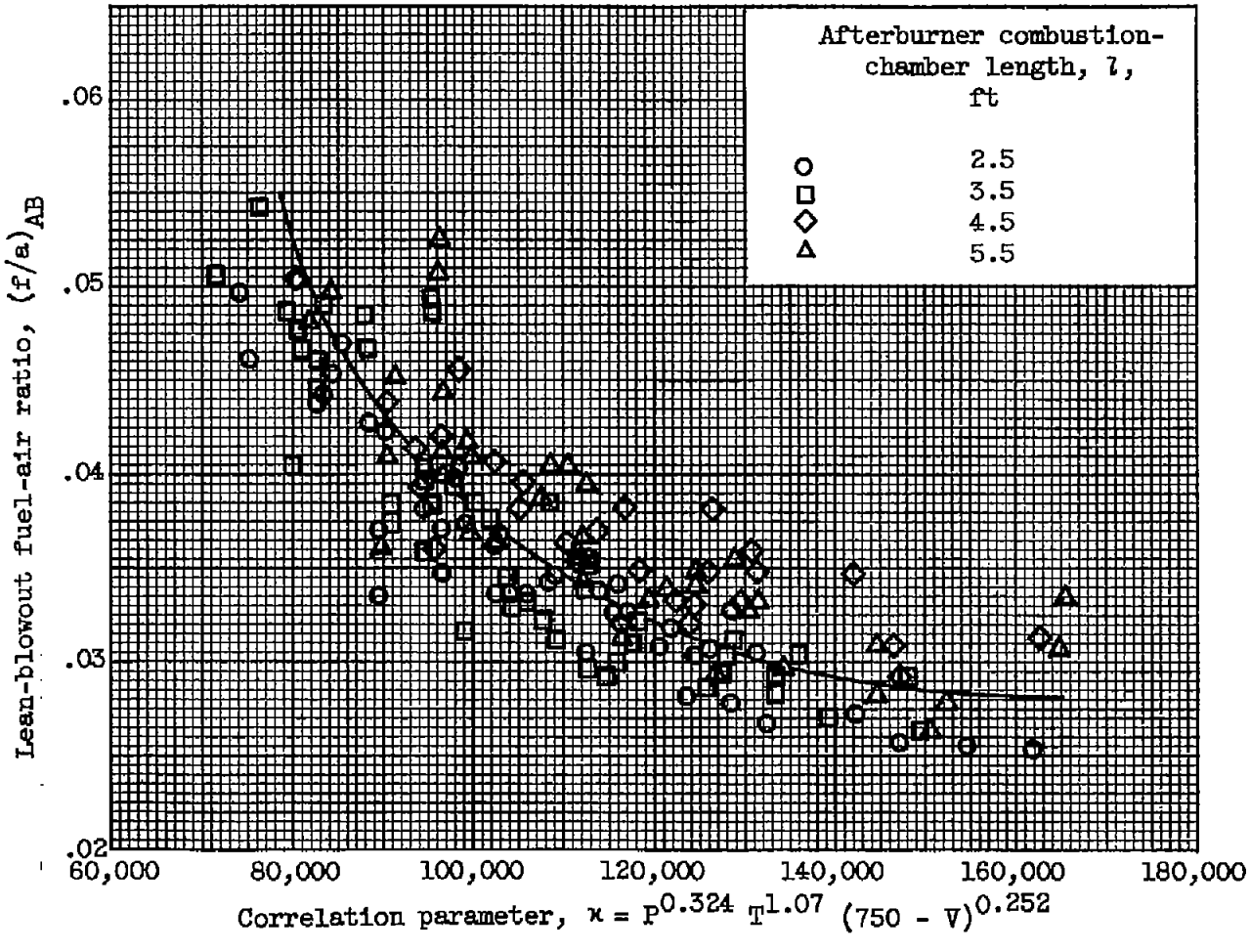

Figure 7. - Correlation of lean-blowout fuel-air-ratio data for several afterburner lengths. Afterburner-inlet total temperatures, 1260° to 1860° R; afterburner-inlet total pressures, 750 to 1800 pounds per square foot absolute; afterburner-inlet velocities, 400 to 650 feet per second.